Passive Acoustic Sensor Network Localization; Application to Structure geometry Monitoring

Vincent Rémy, Carmona Mikael, Olivier Michel, Jean-Louis Lacoume

7th European Workshop on Structural Health Monitoring
July 8-11, 2014. La Cité, Nantes, France

PASSIVE ACOUSTIC SENSOR NETWORK LOCALIZATION; APPLICATION TO STRUCTURE GEOMETRY MONITORING

Rémy VINCENT[1,2], Mikael CARMONA[1], Olivier MICHEL[2] and Jean-Louis LACOUME[2]

[1] *CEA, Leti, 38054 Grenoble, France*
[2] *GIPSA-lab, BP 46 F-38402 Grenoble Cedex, France*

ABSTRACT

In this article, passive acoustic sensor network localization is presented and applied to geometry structure monitoring. The methodology relies on passive travel-time estimation, which is here defined as the retrieval of an inter-sensor propagation delay, using uncontrolled ambient sources in an homogeneous acoustic propagation medium. Our approach relates to passive linear systems identification through the use of codas correlations to form estimators. We provide practical performances of such estimators and propose two approaches for geometry monitoring, both illustrated in the case of a steel beam.

KEYWORDS : *Passive identification, Travel-time estimation, Sensor network localization, Geometry monitoring*

1. INTRODUCTION

Localization of sensors within a network is a required step for monitoring the geometry of mechanical structures. This monitoring was historically achieved with informative stresses of the structures that were user-controlled and typically relies on Euclidean distances measurements between a controlled source and the sensors, *e.g.* GPS, optical devices, marker based techniques. In this paper, we instead work in passive context, which implies that no controlled sources are used. All sensors embedded in the investigated medium are excited by ambient uncontrolled sources only. In this context, ambient noise appears to be a useful source as long as it is sensed by all or some of the sensors. This approach relates to passive linear systems identification.

Pioneering work in passive identification was conducted in structural health monitoring [6], acoustic [17] and seismology [2]. In structural health monitoring, applications were released to determine structural parameters such as seismic velocity, modal damping and frequencies [6, 9, 13]. Lately, it was even shown in [10] that multi-story building impulse responses can be generated from ambient noise correlations only, from major earthquakes. In this article, the proposed method is different, for it is based on the passive geometry retrieval (shape, angle or curvature) using acoustic ambient noise instead of seismic one. Closest work is [12] with underwater acoustic sensor network localization. The corner stone of the approach resides in accessing the distances between sensors, which we will tackle using indoors aerial acoustic pressure fields.

In [3], Green function retrieval was achieved in acoustics and a discussion was conducted on the damping model: in aerial acoustic, weak viscous damping was retained over constant damping, often applied with seismic wavefields [7]. Our work is presently motivated by distance estimation performances assessment, which is divided in two parts. The first part is about detecting a change in the structure geometry: detection theory allows to set a threshold from the spatial resolution on the estimated inter-sensor Euclidean distances, which corresponds to a certain false alarm rate. The second part is about assessing structural parameters of the monitored structure, from the sensor network geometry, such as maximum curvature, maximum bending or Young modulus.

The article is organized as follows: in section 2, passive travel-time estimation theory is introduced. Performances of such estimators in aerial acoustics are derived and discussed. Experimental

performances of distances estimation is conducted with a 7-microphones network and results are presented in section 3. This setup is extended to the two suggested approaches to passive monitoring: passive detection of changes in the sensor geometry and passive shape retrieval. The paper eventually ends summarizing pros and cons of the approach. As for the perspectives, suggestions are made to reach even better accuracy.

2. PASSIVE TRAVEL-TIME ESTIMATION

2.1 Passive/Active context

In an active context, travel-time estimation relies on a controlled transmitter and receiver. The signal transmitted $u(t)$ propagates and is sensed at the receiver as $r(t)$. $r(t)$ is comonly designed as a delayed version of the emitted signal associated with an attenuated amplitude and corrupted by an additive measurement noise: $r(t) = u(t-\tau,\lambda) + b(t)$, where τ is the delay, λ the attenuation and b the noise. The argmax of the correlation between r and u is the natural propagation delay estimator in the sense that it corresponds to the matched filter. Estimation theory then allows to derive a Cramer-Rao lower bound CRLB(τ) on the active travel time estimator, see for instance [21].

In the passive context, sources are not controlled and source signals $r(t)$ are consequently not available. The presented approach tackles the problem from a different angle: second order statistics are used to achieve the passive estimation of impulse responses between sensors in an homogeneous acoustic propagation medium, through the use of Ward identity [3]. Travel-times can then be extracted from those retrieved Green functions.

2.2 Propagation equations and Green functions

Studied media are homogeneous acoustic linear propagation media. Let f be some pressure source field and let s be the corresponding resulting pressure field. In this context, the propagation equation relating f and s has been derived by Stokes [11]:

$$\left[\frac{\partial^2}{\partial t^2} + \eta^2\nabla\frac{\partial}{\partial t} + v^2\nabla\right] f(t,\vec{x}) = s(t,\vec{x}) \tag{1}$$

where η is the viscous-damping coefficient and v the wave celerity. As noticed and shown several times in the literature [3, 7, 17], dissipation has proven necessary in passive estimation theory.

The Green function $G(t,\vec{x}|\vec{y})$ of a linear propagation medium is its impulse response. It stands for the field sensed at $\vec{x}$ at time t, when a pulse was triggered from $\vec{y}$ at time $t = 0$ s. The Green function relates the source and the corresponding response field as a filtering process:

$$f(t,\vec{p}) = \int G(t-t',\vec{p}-\vec{x})s(t',\vec{x})dt'd\vec{x} = (G \underset{T,S}{\otimes} s)(t,\vec{p}) \tag{2}$$

where $\otimes_{T,S}$ stands for the generalized convolution in both time and space. When the medium is homogeneous with a low damping coefficient and in the high-frequency regime [18], the Green function writes as a sum of delays with corresponding attenuated amplitudes:

$$G(t,\vec{p}|\vec{x}) = \sum_{n\leq 0} a_n\delta(t-t_n) \tag{3}$$

where δ is the Dirac distribution, a_n are the damping coefficients and t_n are the delays. The first delay is the time of arrival:

$$t_0 = \frac{r}{v} \tag{4}$$

where r is the Euclidean distance between $\vec{p}$ and $\vec{x}$.

2.3 Green correlation

In the passive context, sources are unknown stochastic processes. While propagating, their wavefronts are shaped by the medium; filtering induces information on the medium which is sensed in the field. To extract this information, the presented approach relies on Ward identity for which the framework deals with 2^{nd} order statistics of the sensed fields.

Let $\gamma_f(\tau,\vec{x},\vec{y})$ be the cross-correlation function of a stochastic and stationary field f at two locations $\vec{x}$ and $\vec{y}$:

$$\gamma_f(\tau,\vec{x},\vec{y}) = \mathbb{E}\left[f(u,\vec{x})f(u+\tau,\vec{y})\right] \tag{5}$$

Combining eq. (2) and (5) gives rise to a generalized interference formula, relating the auto-correlation function of field f generated by a source at $\vec{s}$, to the signals sensed at two locations $\vec{x}$ and $\vec{y}$:

$$\gamma_f(\tau,\vec{x},\vec{y}) = \left[C \underset{T,S}{\otimes} \gamma_s\right](\tau,\vec{x},\vec{y}) \tag{6}$$

where:

$$C = G \underset{T,S}{\otimes} G^{-} \tag{7}$$

and where $G^{-}(t,\vec{x}|\vec{y}) = G(-t,\vec{y}|\vec{x})$ is the time reversed Green function. C is called Green correlation and in equation (6), it is the auto-correlation function of the pressure field generated by a spatio-temporal white source (*i.e.* $\gamma_s(\tau,\vec{x},\vec{y}) = \delta(\tau)\delta(\vec{x}-\vec{y})$). Passive identification is then achievable provided sources are white in time and space, as in (6) information on the medium only remains.

In practice, ambient sources are used, which are barely white even within finite spectral bandwidth. However, seismologists [2] have experimentally shown that the cross-correlations of **codas** of seismic events resulted in a good approximation of the cross-correlation of a propagated white noise.

This results is still true for acoustic propagation media. In Fig. 1, an instance of acoustic coda is displayed; it is a chunk of the field generated by an uncontrolled impulse source. Note that rigorous definition of the coda is difficult and that we thus base its extraction quite similarly to [2], with a power-based rule. Furthermore, a model of the coda was proposed in [2] which allows to locate information in the phase of the coda. As a consequence, one-bit coda signals will be legitimately processed in the passive identification protocol. Note however that 1-bit correlations are distorded versions of the theoretical correlations. Corresponding correction is found in [8], see eq. (8):

$$\gamma_s(\tau) = \sin\left(\frac{\pi}{2}\gamma_{\bar{s}}(\tau)\right) \tag{8}$$

where for signal s, γ_s is its theoretical auto-correlation function and $\gamma_{\bar{s}}$ its normalized 1-bit quantized version. In practice, it is clear that 1-bit quantification ease practical deployment in terms of data transmission, data storage and computation time. Note that 1-bit quantification furthermore preservs the argmaximum position, which is a fundamental property to our purpose.

2.4 Ward identity and travel-time retrieval

The Green correlation is now related to the Green function with the use of a Ward identity [17]. In the acoustic framework and for a low viscous damping, the Ward identity writes [3]:

$$\frac{\partial^3}{\partial t^3}\gamma_G(t,\vec{x},\vec{y}) = \frac{1}{\eta}\gamma_s(t,\vec{s}) \underset{T,S}{\otimes} \mathrm{Odd}\Big[G(t,\vec{x},\vec{y})\Big] \tag{9}$$

where the third time derivative and parameter η are dependent of the viscous-damping model.

From Ward identity (9), one can observe that Green function can be retrieved from an estimation of the Green correlation. Because the air is weakly viscous, the notion of travel-time is preserved

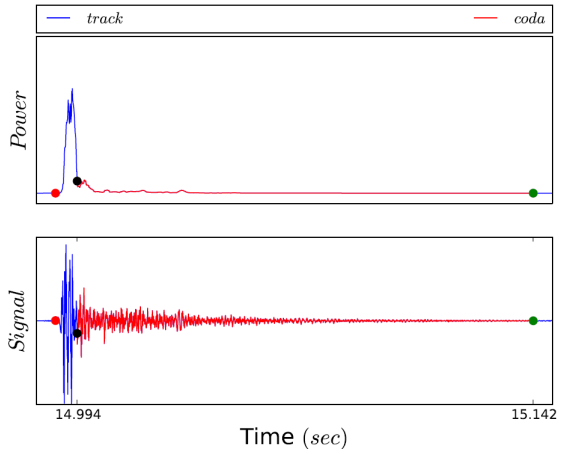

Figure 1 : Instance of acoustic codas

The red dot informs that an acoustic event is detected (hand-clap). The black dot specifies the start of the part of the signal that will be used for identification. The green dot ends the codas as the signal to noise ratio reaches some threshold. Thresholds on the power of the signal were used to process codas extractions. Each coda is then 1-bit quantized. Sub-codas are formed from them, with a sliding window of given length and overlap. These sub-codas are used to perform estimation for each pair of sensors.

through the reconstruction of the Green function expressed in (3). As a consequence, an estimator of the travel-time will be the maximum argument of the estimated Green function. This is illustrated in Fig. 2, where a reconstructed Green correlation and retrieved Green function are displayed, between two microphones with sampling frequency $51kHz$.

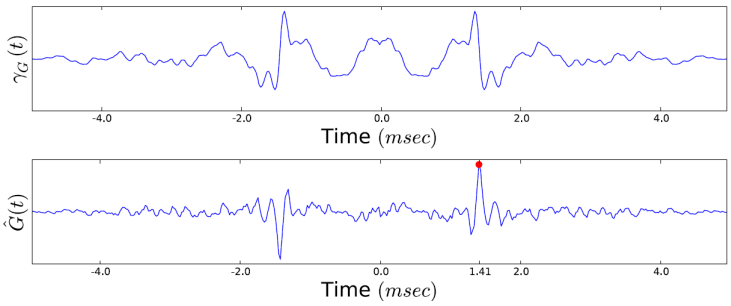

Figure 2 : Retrieved Green function and travel-time

In this example, sensors were $48cm$ away from each other. Amplitudes are normalized. 0.25 seconds of codas were used to compute 1-bit Green correlations and process identification. The dot stands for the result of the passive travel-time estimation: $1.41ms$, which leads to an estimated distance of $48.36cm$.

3. Performances and applications to structural geometry monitoring

3.1 Resolution, convergence and variance

Performances of passive travel-time estimation will now be discussed in an air acoustic propagation medium. Sensors are omnidirectional microphones sampled at $51kHz$.

Sound celerity is $343m/s$ when temperature is $20°C$. The spatial resolution thus is $6.2mm$ at $51kHz$. It goes down to $6mm$ at $10°C$ and up to $6.3mm$ at $35°C$. Note that the influence of altitude is even more negligible.

Codas are noises of interest. They are to be opposed to actual noises with respect to estimation; they can be described as parts of signals that are only seen by either one of the sensors. However, although cross-correlations of these latter are expected to interfer with travel-time extraction, it is only true at very small propagation times. The decay of their correlation function is indeed generally strong.

Acoustic codas are temporally white with a bandwidth that, in our case, is larger than the sampling rate. It is a basic setup in which, Shanon-Nyquist sampling requisite is hardly met as increasing sampling frequencies can raise technological issues. Note that this estimator is created from the sampling of the continuous estimator of the travel-time which has a bias. This latter is expected to be

upper-bounded by the spatial resolution. If not, one can assess that misdetection occured. The estimator can be computed so that its variance reaches the order of magnitude of the spatial resolution. However, the numerical computation leads to a variance that has some properties:

- Correlations are approximated, with residues that have a variance that decreases proportionnaly to the number of points they were computed on;
- The Green correlation is an average of N correlations of the type above, which leads to a corresponding variance that decreases proportionaly with N.
- Eventually, the Green function is estimated from the 3rd-time differenciation of the Green correlation. One can show such numerical differenciation multiplies the variance by 20.

As shown in Fig. 2, we experimentally noticed that 250 averaged correlations to form the Green correlation, from typically $0.25sec$ of 1-bit codas, with sampling frequency $f_s = 51kHz$, lead to 2 likely values for n (others are very unlikely events and will consequently be discarded). Because of this, it means that detection fails $\mathscr{H}_0$ or succeeds $\mathscr{H}_1$, such that:

$$\begin{array}{ll} \mathscr{H}_0 : \mu \geq 1/f_s & \text{misdetection} \\ \mathscr{H}_1 : \mu \leq 1/f_s & \text{detection and } \sigma \leq \frac{1}{6f_s} \end{array} \tag{10}$$

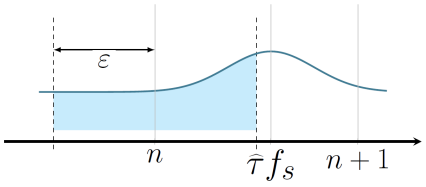

Figure 3 : Travel-time estimator

The continous travel-time estimator has an actual variance that is of the same magnitude than the resolution ε. The actual digital estimator for the travel-time takes only a couple of discreet values. In the figure, the area of the shaded patch for instance stands for the probability that sample n is picked as travel-time estimate. Note that actual $\widehat{\tau}$ is shifted from the actual travel-time τ by a possible bias of the estimator μ.

3.2 Extension to a sensor network: from distances to positions

Let us now raise the reasoning to a sensor network of n sensors. For each pair of sensors, inter-sensor distance ought to be estimated. This leads to a maximum count of $(n-1)(n-2)/2$ inter-sensor distances accessible. These distances can be concatenated in a symmetric matrix $\widehat{D}$, where $\widehat{D}_{ij}$ is the estimated distance between sensor i and sensor j. Because these distances were estimated with performances described above, some additive estimation residue matrix B is used to express the estimation:

$$\widehat{D} = D(X) + B \tag{11}$$

where $D(X)$ is the actual distances matrix, function of positions in matrix X.

Also, note that from a practical point of view, it is realistic to account for the fact that distances may remain unestimated or badly done so. This is accounted for by using adjacency matrix A where A_{ij} is a coefficient in between 0 and 1 which basically relates how confident the estimation is. It is for instance 0 if the distance couldn't be estimated and 1 if estimation protocol succeeded. Eventually, a model of the estimated distance can write using the Hadamar product $\otimes$:

$$\widehat{D} = A \otimes (D(X) + B) \tag{12}$$

In equation (12), assessing the sensor positions X is an inverse problem. Various algorithms are available, one of them being Torgerson's algorithm [15]. Note that in our case, the adjacency matrix A has coefficients that either are 1 (detection) or 0 (misdetection). When matrix A displays unrecovered distances, Kruskal's algorithm [4] can be used to achieve positions estimations. Relative positioning

of the sensor network can become asbolute with the use of anchors. Eventually, the sensor network geometry grants access to parameters such as curvatures, angles or bendings. Estimation errors in the distances will then have an impact on the estimated parameters, whose performances study is very particular to the applications.

We illustrate the argumentation with the example of a beam. The beam is 3m long, doubly supported at 1m from each extremities. It is made of steel, has a Young modulus $E = 210e6N/m$ and quadratic moment $I = 3.9 \times 10^{-8}m^4$. Fig. 4 displays the experimental setup. Sampling frequency is $51kHz$ with corresponding spatial resolution $6.2mm$. Events are handclaps and codas are extracted as introduced in fig. 1.

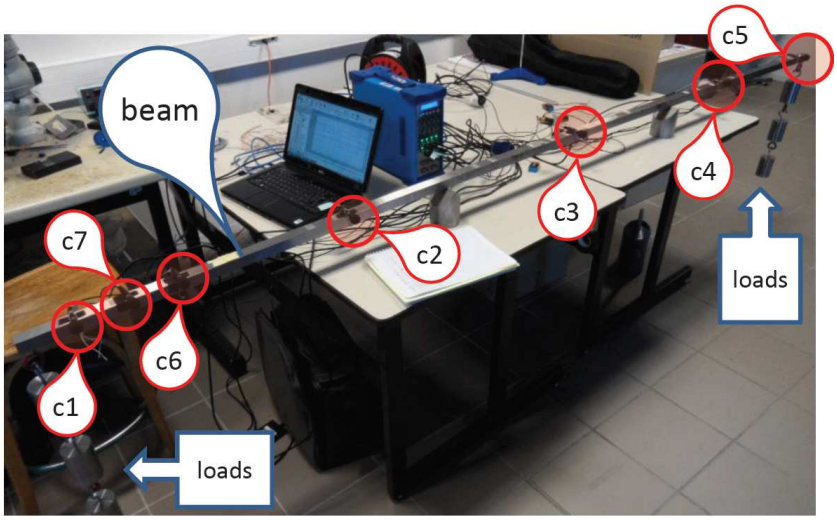

Figure 4 : Beam setup

Below are distance estimation results for the 7 sensors. In (13), inter-sensor distances are displayed, corrupted by the estimation residue (in red). All lengths are expressed in centimeters. Passive travel-time estimation was processed 100 times and the displayed estimation residues result from the average of the discreet estimated values, weighted by their empirical occurance probability.

$$\begin{array}{c} \\ c1 \\ c2 \\ c3 \\ c4 \\ c5 \\ c6 \end{array} \begin{array}{c} \begin{array}{ccccccc} c1 & c2 & c3 & c4 & c5 & c6 & c7 \end{array} \\ \begin{pmatrix} 0 & 60{+}0.4 & 140{-}0.1 & 220{-}0.1 & 280{-}98.5 & 20{+}1.3 & 10{+}0.6 \\ & 0 & 80{+}1.6 & 160{+}0.2 & 220{+}0.5 & 40{-}0.6 & 50{-}0.3 \\ & & 0 & 80{+}0.3 & 140{+}0.6 & 120{+}0.1 & 130{+}0.7 \\ & & & 0 & 60{+}0.7 & 200{+}0.4 & 210{-}1.1 \\ & & & & 0 & 260{-}0.7 & 270{-}1.4 \\ & & & & & 0 & 10{-}0.1 \end{pmatrix} \end{array} \quad (13)$$

Practically speaking, acoustic codas successfully allow to retrieve distances at scales of a 'standard' room, from a centimeter to a few meters. In this study case, the beam dimensions allowed to retrieve all but 1 distances within a centimetric precision. It is not clear to us why the distance estimation between sensor 1 and 5 consistently failed.

3.3 Applications in bending detection and retrieval

3.3.1 Detection

In the first approach, extremities of the beam are loaded and the goal is to characterize the detectability of a change in the geometry of the beam. In this setup, sensors at each extremity of the beam are the

ones that are most influenced by a change in the geometry from loads. As a consequence we will investigate a change in the distance between those two sensors and identify detectability of a bend. Fig. 5 displays the evolution of the equivalent change in the bending given 10 kg loads and a varying Young modulus.

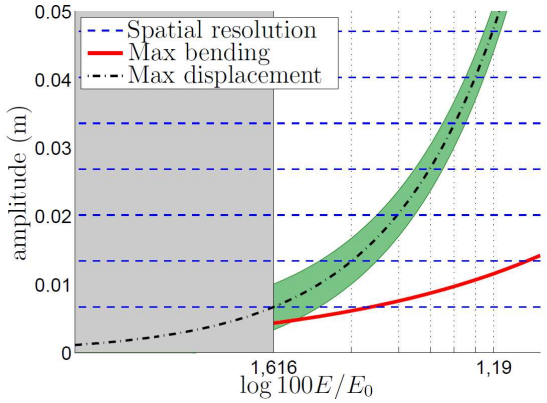

Figure 5 : bending and detection

At a sampling rate of $51kHz$, spatial resolution is $6.2mm$. At given loads equal to $10kg$, sensors would become this quantity closer when the Young modulus gets below $0.39E_0$. Corresponding maximum bending is located in the middle of the beam and is $4.3mm$. A bend in this beam thus becomes detectable after this threshold. The shaded area in the figure is the area where a bend is not detectable as it would be subresolution. The next detectable bends have corresponding bending that are millimetric.

3.3.2 Evaluation

For the second approach, sensors are located in the medium with no control. The approach had now better rely on reconstructing the geometry of the beam. Fitting splines from retrieved sensor positions is an instance on how to achieve it in 2 dimensions. Fitting surfaces would be the extension in 3 dimensions. We now provide an example of geometry reconstruction, see fig. 6.

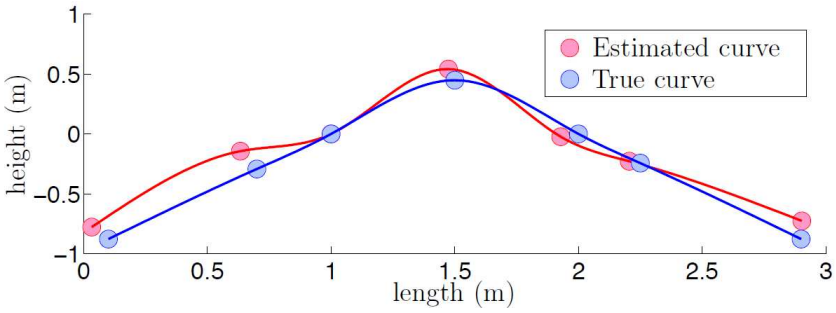

Figure 6 : bending and detection

The inverse problem that relates distances to positions proves to be very sensitive to the variance of distances estimation. Given a $6.2mm$ spatial resolution and a variance of the same magnitude, we display the result of meter-wise geometry retrieval. Variance in the positions estimation is centimetric, which prevents to use this configuration to assess the maximum bending of the beam from 4. This variance will however allow relevant applications at larger scales, *e.g.* for the monitoring of a vault. Any multi-dimensional scaling approach used for this inverse problem should be characterized through the evolution law that relates the variance in the positions σ_X^2 to the variance in the distances σ_D^2. Although it may be described by very specific parameters, which depends on the study case, a general remark is that $\sigma_X^2 \geq \sigma_D^2$. Geometrical parameters to be estimated from the reconstructed geometry should then be of a much bigger order of magnitude in order for the estimation to be make sense.

4. CONCLUSIONS AND PERSPECTIVES

Performances of passive travel-time estimation have been presented in the air acoustic framework. Experiments have shown that the standard deviation of the estimator is lower than the sampling frequency. Thus, with a sampling at 51.2 kHz, accuracy is better than the centimeter. This performance allows to retrieve the geometry of a sensor network distributed at larger scales.

However, calculus derived in the context of an instrumented steel beam show that accuracy needs to be improved to detect changes and to retrieve the shape (or the bending) with an acceptable precision. Thus, two extensions are under investigation. The first one is related to the theoretical study of Green correlation retrieval with codas; even if the passive identification protocol works, all parameters are not entirely understood. Extraction of codas is probably the most probant one.

Secondly, experimentations with a higher sampling frequency will naturally improved the accuracy of the travel-time retrieval and will allow to discover the real limit of the estimation for the moment limited by technology.

REFERENCES

[1] Aki, K., and P. G. Richards (1980). *Quantitative Seismology: Theory and methods*, W. H. Freeman, San Francisco, California, 161187.

[2] M. Campillo, A. Paul, *Long-range correlations in the diffuse seismic coda*, Science 299 (2003) 547-549.

[3] M. Carmona, O. Michel, J-L. Lacoume, B. Nicolas, N. Sprynski, *Ward identities for visco-acoustic and visco-elastic propagation media*, Wave motion 49 (2012) 484-489.

[4] Kruskal, J. B. (1956). *On the shortest spanning subtree of a graph and the traveling salesman problem*, Proceedings of the American Mathematical Society 7:48-50.

[5] O. Lobkis, R. Weaver, On the emergence of the Green function in the correlations of a diffuse field, J. Acoust. Soc. Am. 110 (2001) 3011-3017.

[6] C. R. Farrar, G. H. James III, *System Identification from Ambiant Vibration Measurements on a Bridge*, Journal Sound and Vibration 1, 1999.

[7] P. Gouedard, L. Stehly, F. Brenquier, M. Campillo, Y. Colin de Verdiere, E. Larose, L. Margerin, P. Roux, F. J. Sanchez-Sesma, N. M. Shapiro, R. Weaver, *Cross-correlation of random fields: mathematical approach and applications*, Geophysical Prospecting 56 (2008) 375-393.

[8] B. Pincinbono, *Sur certains problèmes concernant la détection des signaux faibles*, Annales des Télécommunications, 1961, Tome 16, 12.

[9] G. A. Prieto, *Anelastic Earth structure from the coherency of the ambient seismic field*, Journal of Geophysical Research, vol. 114, B07303, 2009.

[10] Prieto, G. A., J. F. Lawrence, A. I. Chung, and M. D. Kohler (2010). *Impulse response of civil structures from ambient noise analysis*, Bull. Seismol. Soc. Am. 100, 23222328.

[11] D. Royer, E. Dieulesaint, *Elastic Waves in Solids*, Springer 2000.

[12] K.G. Sabra, P. Roux, A.M. Thode, G.L. D'Spain, W.S. Hodgkiss, W.A. Kuperman, Using Ocean Ambient Noise for Array Self-Localization and Self-Synchronization, IEEE J Oceanic. Eng. 30 (2005) 338-347.

[13] Snieder, R., and E. Safak (2006). *Extracting the building response using seismic interferometry: Theory and application to the Millikan Library in Pasadena, California*, Bull. Seismol. Soc. Am. 96, 586598.

[14] Snieder, R., S. Hubbard, M. Haney, G. Bawden, P. Hatchell, and A. Revil DOE Geophysical Monitoring Working Group (2007). *Advanced non-invasive geophysical monitoring techniques*, Ann. Rev. of Earth Planet. Sci. 35, 653683.

[15] Torgerson, Warren S. (1958). *Theory & Methods of Scaling*. New York: Wiley. ISBN 0-89874-722-8.

[16] K. Wapenaar, E. Slob, R. Snieder, A. Curtis. *Tutorial on seismic interferometry, part II : underlying theory and new advances*. Geophysics 75 (2010) 75A211-75A227.

[17] R. Weaver, *Ward identities and the retrieval of Green's functions in the correlations of a diffuse field*, Wave Motion 45 (2008) 596-604.

[18] M. Wright, R. Weaver, *New Directions in Linear Acoustics and Vibration, Quantum Chaos, Random Matrix theory and Complexity*. Campbridge University Press.

[19] Yao, H., R. D. van der Hilst, and M. V. de Hoop (2006). *Surface-wave array tomography in SE Tibet from ambient seismic noise and two-station analysis I. Phase velocity maps*, Geophys. J. Int. 166, 732744.

[20] Zheng, S., X. Sun, X. Song, Y. Yang, and M. H. Ritzwoller (2008). *Surface wave tomography of china from ambient seismic noise correlation*, Geochem. Geophys. Geosyst. 9.

[21] J. Ziv, M. Zakai, *Some Lower Bounds on Signal Parameter Estimation*, IEEE Transactions on Information Theory 15, 1998.